*Environ. Sci. Technol.* **2006**, *40,* 7694−7701

# Sorption of Trichloroethylene in Hydrophobic Micropores of Dealuminated Y Zeolites and Natural Minerals

HEFA CHENG AND MARTIN REINHARD*

*Department of Civil and Environmental Engineering, Stanford University, Stanford, California 94305-4020*

Sorption of volatile organic compounds (VOCs) in low organic carbon (<0.1%) geosorbents is difficult to predict because the sorption capacity of the mineral matrix is poorly understood. This research demonstrates hydrophobic micropores can be important sorption sites for VOCs. We studied the sorption of water and TCE on three dealuminated Y zeolites ranging from hydrophilic (CBV-300) to hydrophobic (CBV-720 and CBV-780), with the surface cation density decreasing from 2.07 to 0.42 and 0.16 sites/nm$^2$, respectively. Water sorption and dehydration data indicate water affinity of the zeolite micropores decreases with micropore hydrophobicity. TCE sorption on the wet zeolites decreased with increasing surface cation density. At a relative pressure ($P/P_0$) of 0.136, TCE filled only 0.034% of the micropore volume in wet CBV-300, but 16.9% and 18.6% in wet CBV-720 and CBV-780, respectively. TCE desorption data from dry and wet silica sand (Min-U-Sil 30), kaolinite (KGa-1), and smectite (SWy-1) confirmed VOC sorption in wet microporous minerals is controlled by both the micropore volume and hydrophobicity. Results suggest TCE adsorbs in hydrophobic micropores by displacing loosely bound water, consistent with the theoretical considerations indicating the process of transferring loosely bound water from hydrophobic micropores to the bulk phase is energetically favorable.

## Introduction

Micropores (pores with diameters ≤2 nm) in synthetic sorbents (e.g., silica gels and zeolites) and geosorbents (aquifer materials, soils, and sediments) strongly sorb and slowly release volatile organic compounds (VOCs), such as trichloroethylene (TCE), even in the presence of water (*1*−*5*). Adsorption in micropores of geosorbents is an important factor influencing the transport of organic contaminants in the subsurface (*1*, *2*, *4*). Sorption of VOCs in micropores in the presence of water is believed to be governed by the hydrophobicity of the micropores (*5*). Hydrophobic micropores are pores with hydrophobic surfaces characterized by a low density of hydrophilic centers (surface cations and surface-bound hydroxyl groups) and weak interactions with water molecules. Mineral components of geosorbents have been recognized to be microporous (*1*, *2*, *6*); a recent study suggests that the microporosity of geosorbents resides mainly in clays (phyllosilicates) (*6*). A small fraction of the micropores in geosorbent minerals can be hydrophobic, exhibiting a strong affinity for hydrophobic contaminants (*5*). To study the effect of micropore hydrophobicity of VOC sorption without the confounding effect of organic carbon, we studied three crystalline dealuminated Y zeolites and three natural minerals as model systems for micropores in silicate minerals.

Although zeolites occur rarely in geosorbents, they were chosen as model sorbents because of their high microporosity, well-defined pore structure, and hydrophobicity. Zeolites are crystalline, microporous aluminosilicates with an infinitely extending three-dimensional framework of $SiO_4$ and $AlO_4$ tetrahedra linked together by sharing the oxygens (*7*). Each $AlO_4$ tetrahedron bears a net negative charge balanced by a cation attracted to, but not actually part of, the crystal structure. Dealumination (by leaching Al or isomorphous substitution of framework Si for Al, Supporting Information) decreases the framework surface charge and removes the surface cations (*8*). During this process, neighboring silanol groups undergo cross-condensation, forming nonpolar or hydrophobic siloxane surfaces (*8*, *9*). Consequently, zeolites with higher silica contents are more hydrophobic; transition of dealuminated zeolites from hydrophilic to hydrophobic occurs at Si/Al ≈ 8 (*10*).

Hydrophilic centers formed by either silanol groups or cations associated with the tetrahedrally coordinated aluminum dominate the adsorption of water in zeolite micropores (*8*, *11*), as indicated in Figure 1. Cations located at the surface of zeolite pores form coordinated covalent bonds with water (coordinated water) (*7*, *11*), while water hydrogen bonded to either silanol groups or coordinated water molecules is termed "zeolitic water" (*7*, *12*). In the absence of strong interactions, pores of zeolites are filled by water via capillary condensation requiring a relative pressure ($P/P_0$) of nearly 1 (*13*). Water condensed in hydrophobic pore spaces is termed "loosely bound" water (*14*). Compared to bulk water, loosely bound water is more disordered because the molecules are not coordinated or hydrogen-bonded in fixed positions and is therefore released easily upon heating (<100 °C) (*14*, *15*). Removal of zeolitic water can be achieved by exposure to vacuum or by heating to approximately 100 °C; coordinated water requires more extreme conditions (e.g., >350 °C or constant vacuum pumping) (*16*). For zeolites with a high density of surface cations, coordinated water can completely fill the micropore spaces, leaving little room for hydrogen-bonded or loosely bound water (*8*).

The effect of micropore hydrophobicity on water and organic sorption in microporous carbon has been studied experimentally and by molecular simulations. In graphite micropores, nonpolar vapors such as methane are strongly sorbed, even at very low pressures because dispersion interactions are enhanced in the narrow pore spaces (*13*, *17*, *18*). In contrast, pore filling by water requires a $P/P_0$ of nearly 1 because hydrogen bonding between water molecules is restricted in hydrophobic micropores (*17*−*19*). Both experimental and molecular simulation results show that hydrogen-bonding sites greatly enhance adsorption of water in carbon micropores (*13*, *17*, *19*). Molecular simulations show that, for adsorption of water/methane mixtures into a carbon micropore, methane is strongly preferred in the absence of hydrogen-bonding sites, and that the adsorption of water rises rapidly as the hydrogen-bonding site density increases (*17*, *20*). A molecular simulation study on adsorption of water/methanol mixtures indicates that uncharged aluminosilicate micropores are even more hydrophobic than graphite micropores (*18*). Molecular simulation also showed that water significantly decreases TCE adsorption in hydrophilic

* Corresponding author phone: (650) 723-0308; fax: (650) 723-7058; e-mail: reinhard@stanford.edu.



10.1021/es060886s CCC: $33.50 
Published on Web 10/31/2006

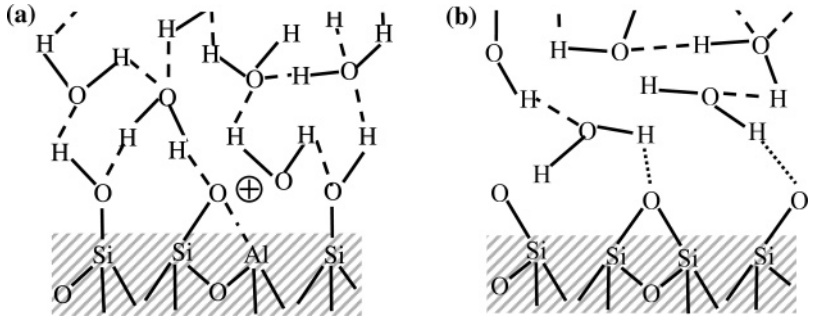


**FIGURE 1. Structure of water molecules in a hydrophobic zeolite micropore: (a) In hydrophilic pore spaces, water molecules arrange with well-defined orientations and stay at fixed positions surrounding the hydrophilic centers (surface cations and silanol groups) on the pore wall surface through both electrostatic interactions and hydrogen bonding. "⊕" represents a surface proton or cation such as $Na^+$ or $NH_4^+$ electrostatically attached to the surface. (b) In hydrophobic pore spaces, water−surface interactions are weak and water molecules form disordered clusters through limited intermolecular hydrogen bonding. Water only forms weak hydrogen bonds with the hydrophobic siloxane surface.**

(charged) silica micropores but that it has a small effect in mildly hydrophobic (uncharged) pores (*21*).

This research examined the hypothesis that sorption of VOCs, specifically TCE, in micropores is governed by micropore hydrophobicity. The approach was to first quantify TCE sorption in three structurally identical zeolites of varying hydrophobicity at different water contents. The hypothesis was further tested with three natural minerals common in geosorbents: two clays, kaolinite (KGa-1) and smectite (SWy-1), and a silica sand (Min-U-Sil 30).

Because of the irregular nature of the clay crystals, especially the distribution of crystal thickness and terraced surfaces, stacking of the crystals and quasicrystals can create interparticulate micropores (*22*, *23*). In kaolinite, micropores are mainly present in the relatively small number of cuneiform voids because of the thick (∼100 nm) plates (*24*). The presence of micropores in smectites is primarily due to turbostratic stacking of elementary layers in tactoids, which creates slit-shaped micropores with sizes corresponding to the thickness of one to several smectite layers (1 nm) on the broken edges of the layers (*25*). However, the thin lamellae of smectite are subjected to large forces during drying, leading to massive deformation and prevalence of cuneiform voids within the remaining microporosity (*24*). Min-U-Sil 30 is expected to have very low microporosity, resulting from possible cracks and pits on the particle surface due to weathering and grinding (by the manufacturer), and interparticulate void spaces of the roughly spherical grains. Of the three natural minerals, only SWy-1 has permanently charged surfaces and predominantly hydrophilic micropores.

## Thermodynamic Considerations

Water molecules sorbed in mineral micropores exhibit a range of stabilities. In micropores of zeolites, water molecules coordinated to surface cations (hundreds of kilojoules per mole) are most stable, followed by water molecules hydrogen bonded to coordinated water or silanol groups (∼20 kJ/mol) (Figure 1a) and loosely bound water. Loosely bound water interacts weakly with the siloxane surface and lacks a significant fraction of intermolecular hydrogen bonding present in bulk water (Figure 1b). At room temperature, the thermal energy (∼2.5 kJ/mol) and the energies of van der Waals interactions (∼2−4 kJ/mol) of organic molecules, such as TCE, are strong enough to displace loosely bound water from micropores. The estimated enthalpy change of transferring loosely bound water from hydrophobic pores to bulk water is approximately −11.3 kJ/mol (*26*). The entropy of loosely bound water in zeolite pores is 7−12 J/(mol K) (or 2.1−3.6 kJ/mol at 25 °C) lower than that of bulk water under standard conditions (*14*). Hence, loosely bound water is relatively unstable.

Dissolved TCE ($TCE_{diss}$, 0.15 $nm^3$/molecule) adsorbs from aqueous solution into hydrophobic micropores, where it forms a bulklike phase ($TCE_{cond}$) (*13*), with the loosely bound water ($water_{loose}$, 0.03 $nm^3$/molecule) being displaced into the bulk phase ($water_{bulk}$). These processes (Supporting Information) can be written as

$$TCE_{diss} + 5\ water_{loose} \Rightarrow TCE_{cond} + 5\ water_{bulk}$$

The Gibbs free energy change ($\Delta G$) associated with transferring dissolved TCE into water-filled micropores is the sum of an enthalpy term, $\Delta H$, and an entropy term, $-T\Delta S$:

$$\Delta G = \Delta H - T\Delta S$$

The entropic contribution ($-T\Delta S$) to the excess free energy of solution for TCE in water is 20−26 kJ/mol at 20−25 °C (*27*). Therefore, the net entropic contribution ($-T\Delta S$) of transferring dissolved TCE molecules from bulk water into hydrophobic pore spaces is estimated to range from −2.3 to −15.7 kJ/mol (of TCE sorbed) at room temperature.

Displacing water from hydrophobic micropore spaces into the bulk phase is exothermic because water molecules are transferred from an environment with weak electrostatic interactions to the bulk phase where water−water interactions are strong (*26*). The enthalpic contribution ($\Delta H$) to the excess free energy of TCE solution in water is around −4 to +2 kJ/mol at room temperature (*27*). Consequently, the net enthalpy change ($\Delta H$) of sorption of TCE from aqueous solution is approximately −56 kJ/mol (of TCE sorbed). This value is comparable to the isosteric heat of adsorption (−35 to −64 kJ/mol) observed for TCE sorption in a high-silica zeolite (*3*). The above analysis indicates that in hydrophobic micropores both the enthalpy and the entropy terms favor TCE adsorption although the enthalpic contribution is more significant, consistent with the results of a molecular simulation study by Luo and Farrell (*21*). These authors have shown that, for the competitive adsorption of water and TCE in slit-shaped, uncharged silica micropores, the enthalpic contribution ($\Delta H$) to the total Gibbs free energy associated with TCE adsorption ($\Delta G$) is always greater than or equal to the entropic contribution ($-T\Delta S$).

## Materials and Methods

**Materials.** Table 1 summarizes the properties of the model sorbents used in this study. Binder-free dealuminated Y zeolites (CBV-300, CBV-720, and CBV-780) were obtained from Zeolyst (Valley Forge, PA) in powder form (1−2 $\mu$m diameter crystals). These zeolites have reproducibly controllable physical and chemical characteristics and crystallinity close to that of their nondealuminated parent zeolites (*28*).

**TABLE 1. Properties of the Dealuminated Y Zeolites and Natural Minerals Used in This Study**

| | Zeolites | | |
|---|---|---|---|
| | CBV-300 | CBV-720 | CBV-780 |
| Si/Al mole ratio[a] | 2.6 | 15 | 40 |
| bulk density, g/cm$^3$ | 1.01 | 1.01 | 1.01 |
| theoretical micropore vol, mL/g | 0.48 | 0.48 | 0.48 |
| nominal cation form[a] | ammonium | hydrogen | hydrogen |
| [$Na_2O$],[a] wt % | 2.8 | 0.03 | 0.03 |
| unit cell size,[a] Å | 24.68 | 24.28 | 24.24 |
| BET surface area,[a] m$^2$/g | 925 | 780 | 780 |
| monovalent cation density,[b] sites/nm$^2$ | 2.07 | 0.42 | 0.16 |

| | Natural Minerals | | |
|---|---|---|---|
| | Min-U-Sil 30[c] | KGa-1[d] | SWy-1[d] |
| composition | 99.5% α-quartz, 0.2% alumina, 0.3% others | 96% kaolinite, 3% anatase, 1% others | 75% smectite, 8% quartz, 16% feldspar, 1% others |
| structure of the major mineral | tectosilicate | 1:1 dioctahedral | 2:1 dioctahedral |
| BET surface area, m$^2$/g | 0.8[e] | 10.0[f] | 31.8[f] |
| particle size, μm | 2 to 40 | 0.1−40[g] | 0.1−0.4[g] |
| CEC,[h] cmol(+)/kg | <3.0[i] | 2.0 | 76.4 |
| layer charge per unit cell [$O_{20}(OH)_4$] | | 0[i] | −0.16 (Tet),[j] −0.52 (Oct)[j] |

[a] From product data sheets of Zeolyst (Valley Forge, PA). [b] Estimated from the Si/Al mole ratios and the general molecular formula of faujasite [$(Mg,Na_2,Ca)_{3.5}[Al_7Si_{17}O_{48}]\cdot 32(H_2O)$] assuming monovalent cations only. [c] From product data sheet of U.S. Silica (Berkeley Springs, WV) unless indicated otherwise. [d] From ref *36*, unless indicated otherwise. [e] Measured by nitrogen gas adsorption in this study. [f] Values reported in ref *36*. [g] Apparent particle sizes reported in ref *37*. [h] The cation exchange capacity (CEC) arises from the permanent charges produced by isomorphous substitutions and/or the induced charges (pH-dependent) that originated from broken bonds at particle edges. [i] The CEC of Min-U-Sil 30, which has a median diameter of 8 μm, should be much smaller than that (3.0 cmol(+)/kg) of Min-U-Sil 5 (median diameter 1.7 μm) (*38*). [j] Tet = tetrahedral and Oct = octahedral, reported in ref *32*.

Y zeolites have the FAU structure (Supporting Information) with pores running perpendicular to each other in the *x*, *y*, and *z* planes, and the pore diameter is large at 7.4 Å with a larger cavity of diameter 12 Å. The estimated densities of monovalent surface cations are 2.07, 0.42, and 0.16 sites/nm$^2$ in the micropores of CBV-300, CBV-720, and CBV-780, respectively. Information on the density of silanol groups is not available. Kaolinite (KGa-1) and smectite (SWy-1) were obtained from the Clay Minerals Society's Source Clays Repository (University of Missouri, Columbia, MO). Ground natural crystalline silica sand, Min-U-Sil 30 (median diameter of 8 μm), was supplied by U.S. Silica (Berkeley Springs, WV). All solids were used without pretreatment.

**Water Sorption and Thermal Dehydration.** Oven-dried zeolites (105 °C for 48 h) were placed in desiccators and equilibrated (>3 months) at room temperature (24 ± 1 °C) with water vapor at ~38%, ~48%, ~90%, and 100% relative humidities (RHs), which were controlled by saturated NaI, $K_2HPO_4$, and $MgSO_4$ solutions and water, respectively (*29*). Water contents were determined by weight losses following stepwise dehydration treatments (Supporting Information). All data reported for water sorption and dehydration are means of triplicate samples. Water sorption on the natural minerals was not investigated because of their small micropore volumes.

**TCE Sorption and Desorption.** TCE was chosen as a representative VOC of this study because it is environmentally relevant and has a relatively low polarity (0.77 D). Solids used for TCE sorption and desorption were either dried at 105 °C for 48 h or hydrated at 100% RH (>3 months). Dried natural minerals were designated as "dry", while zeolites dehydrated incompletely under such conditions and were designated as "partially dehydrated". The apparatus and procedures described elsewhere (*5*) were used to quantify the amounts of TCE sorbed in micropores of the zeolites and natural minerals. In brief, glass columns were first packed with the solids, with the masses determined by column weight differences. Columns packed with the partially dehydrated zeolites or dry natural minerals were reconditioned in a 105 °C oven (without flow), while those packed with the wet solids were purged with a humidified (100% RH) helium stream for at least 2 h. During sorption experiments, the columns of partially dehydrated zeolites or dry natural minerals were fed with a dry helium stream containing TCE vapor at 1.00 mL/min, while a humidified (100% RH) helium stream containing TCE vapor was used for the columns with wet solids. The TCE concentration in the column effluent was quantified using a gas chromatograph with a flame ionization detector (FID) and an electron capture detector (ECD) connected in parallel. The flow was stopped at complete breakthrough, and the column was equilibrated in a 50 °C oven for 10 h after being sealed. To study desorption, the columns were purged with a humidified (100% RH) helium stream at 1.00 mL/min, and the TCE concentration in the purge flow was continuously measured.

**Data Analysis.** The mass of TCE retained in the column was calculated by integrating the area above the sorption breakthrough curve after subtracting the area due to the system dead volume (i.e., the volume in the flow path from the column outlet to the detectors), which was measured by blank runs without columns. Except for wet CBV-300, the amounts of TCE that resided outside of the micropores were minimal relative to those sorbed in the micropores of the zeolites and were thus neglected in mass calculations. For wet CBV-300 and the natural minerals (both wet and dry), the masses of TCE in the micropores were estimated by evaluating the slow-desorbing fractions with a model developed by Li and Werth (*4*) as described by Cheng and Reinhard (*5*). Volumes of the micropores occupied by TCE and water were calculated from their masses on the basis of Gurvitsch's rule by assuming their packing densities in micropores were the same as those of bulk fluids (*13*).

## Results and Discussion

**Water Sorption and Dehydration on Zeolites**. Figure 2a shows the water sorption isotherms of the dealuminated Y zeolites measured between 38% and 100% RH. Water sorption of CBV-300 (surface cation density 2.07 sites/nm$^2$) followed a type I isotherm, with a limiting plateau at approximately

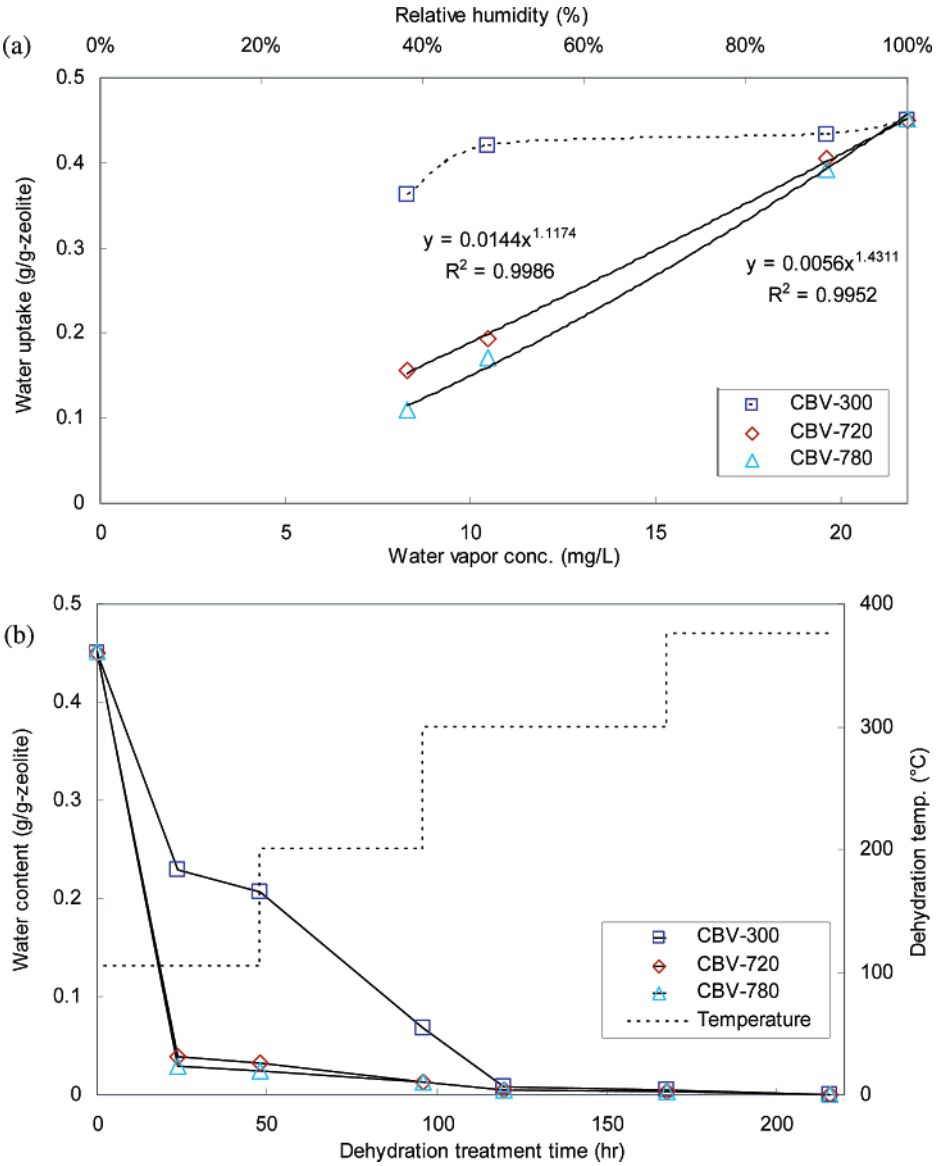


**FIGURE 2. Hydration and dehydration characteristics of three dealuminated Y zeolites: (a) water sorption isotherms at room temperature (24 ± 1 °C); (b) water contents following stepwise thermal dehydration treatment (Supporting Information). Literature data indicate that Y zeolites lose water continuously in the temperature range of 100−400 °C, and the structure is stable up to 760 °C (*7*, *9*). The zeolite dry weights were based on those after dehydration at 375 °C.**

50% RH, indicating that the micropores were nearly filled. Water sorption on CBV-720 and CBV-780 (surface cation density 0.43 and 0.16 site/nm$^2$) exhibited type III isotherms, which are typical for sorbents with weak affinities for the sorbates (water in this case) (*13*, *28*). Water uptake at 100% RH was 0.45 g/g in all three cases, in agreement with the reported values for CBV-780 (0.46−0.47 g/g (*3*)). This value is approximately 6% lower than the void volume fraction of Y zeolites (0.48), probably caused by a slightly lower packing density of water molecules in micropores (*13*, *18*). These findings agree with literature data obtained with dealuminated Y zeolites (*28*) and confirm that pore volumes of Y zeolites are independent of the Si/Al ratio and that water sorption isotherms are influenced by the hydrophobicity (i.e., the density of hydrophilic centers). Similar findings were reported for microporous carbon sorbents (*19*, *20*). The fact that water uptakes of all three Y zeolites at 100% RH are equal to the pore volume of crystalline Y zeolites indicates their structures were not significantly altered by the dealumination process although the presence of small amounts of amorphous mesoporous silica cannot be excluded. Small amounts of amorphous silica would not alter the water sorption isotherms, however.

Figure 2b shows the water losses of the wet zeolites in response to stepwise heating to 105, 200, 300, and 375 °C in 24−72 h increments. As expected, water retention decreased with surface cation density in the order CBV-300, CBV-720, and CBV-780, with the latter two showing only a small difference. The weights of the three zeolites at 375 °C were taken as their dry weights because their water losses at higher temperatures were insignificant. Heating at 105 °C for 48 h removed 92.9% and 94.7% water from CBV-720 and CBV-780, respectively, but only 54.0% from CBV-300. This fraction presumably consists of loosely bound and zeolitic water (*14*, *16*). The amount of water remaining after heating to 105 °C correlates with the surface cation density ($R^2$ = 0.994), indicating that the residual water was probably coordinated to surface cations. Coordinated water was removed at temperatures above 105 °C; only 3−4 mg/g water remained in the zeolites at 300 °C.

**TCE Sorption on Zeolites.** Parts a and b of Figure 3 show the TCE breakthrough curves for the three partially dehy-

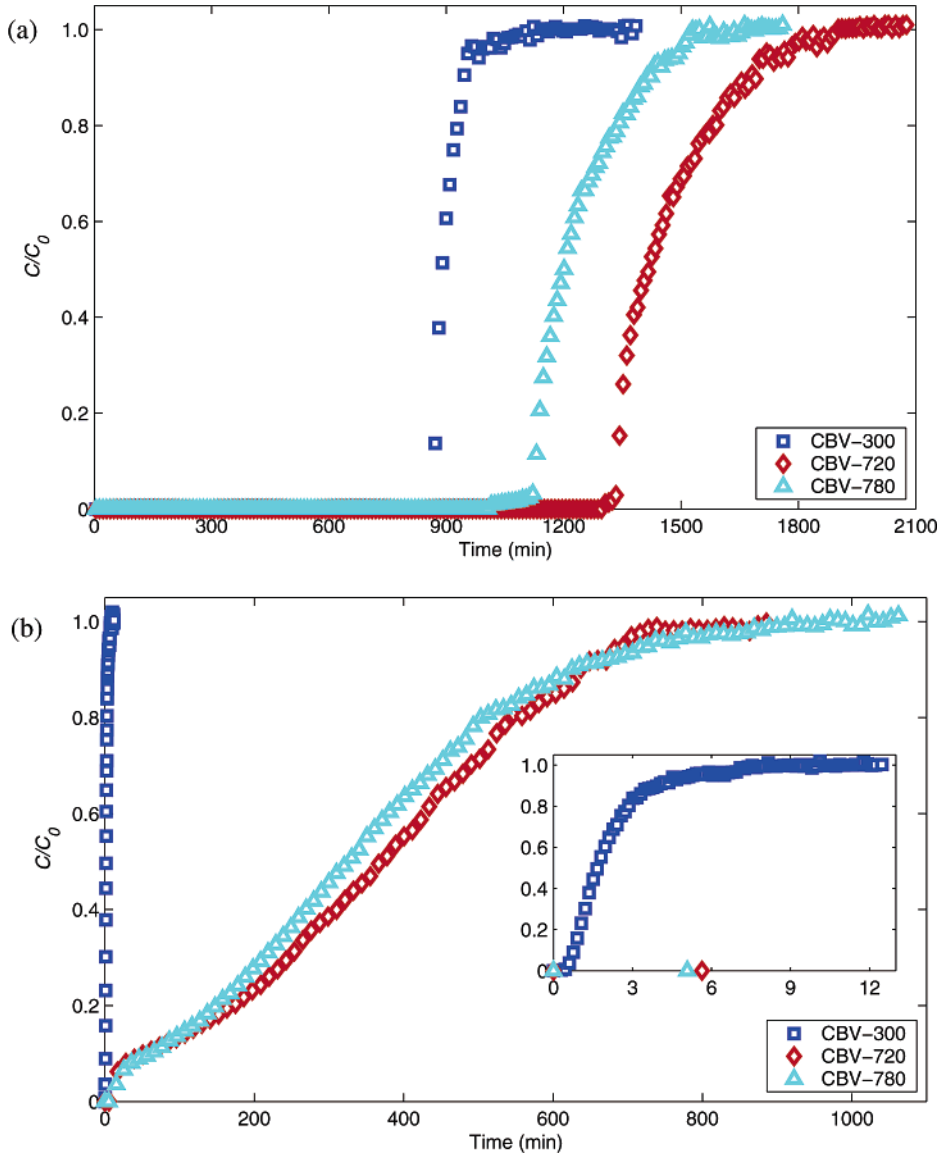


**FIGURE 3. Breakthrough curves of TCE on (a) partially dehydrated and (b) wet CBV-300, CBV-720, and CBV-780 (normalized to 0.2 g of dry solid) at 24 °C, with the inset showing a magnified view for wet CBV-300. The partially dehydrated zeolites had been oven dried at 105 °C for 48 h, while the wet zeolites had been equilibrated at 100% RH. Dry (for partially dehydrated zeolites) or humidified (100% RH, for wet zeolites) helium with TCE vapor ($C_0 = 5.05 \times 10^{-1}$ mmol/L or $P/P_0 = 0.136$) was passed through the column at 1.00 mL/min (~1.4 pore volumes/min) during sorption.**

**TABLE 2. Summary of Volumes of TCE (at $P/P_0 = 0.136$) and Water Sorbed in Micropores of the Partially Dehydrated and Wet Dealuminated Y Zeolites**

| | sorbent = CBV-300 | | sorbent = CBV-720 | | sorbent = CBV-780 | |
|---|---|---|---|---|---|---|
| | partially dehydrated | wet | partially dehydrated | wet | partially dehydrated | wet |
| water content, g/g | 0.21 | 0.45 | $3.2 \times 10^{-2}$ | 0.45 | $2.4 \times 10^{-2}$ | 0.45 |
| water vol,[a] mL/g | 0.21 | 0.45 | $3.2 \times 10^{-2}$ | 0.45 | $2.4 \times 10^{-2}$ | 0.45 |
| amt of TCE sorbed, mmol/g | 2.27 | $1.7 \times 10^{-3}$ [d] | 3.71 | 0.85 | 3.13 | 0.93 |
| TCE vol,[a] mL/g | 0.20 | $1.5 \times 10^{-4}$ | 0.33 | $7.6 \times 10^{-2}$ | 0.28 | $8.4 \times 10^{-2}$ |
| TCE + water vol,[b] mL/g | 0.41 | 0.45 | 0.36 | 0.53 | 0.30 | 0.53 |
| amt of water displaced,[c] mL/g | | $1.5 \times 10^{-4}$ | | $7.6 \times 10^{-2}$ | | $8.4 \times 10^{-2}$ |

[a] Volumes of micropores occupied by TCE and water were calculated by assuming they resided in micropores at the same densities as the bulk fluids. [b] Calculated as the sum of the water volume and TCE volume assuming no water displacement. [c] Calculated as the differences between the total pore volume filled and the water volume for the wet zeolites. [d] Calculated from the mass of TCE desorbed in the slow-desorbing fraction (data not shown).

drated and wet Y zeolites, respectively, and Table 2 summarizes the amounts of water and TCE sorbed. TCE uptakes calculated from the breakthrough curves on partially dehydrated CBV-300, CBV-720, and CBV-780 were 2.27, 3.71, and 3.13 mmol/g, corresponding to TCE volumes of 0.20, 0.33, and 0.28 mL/g, respectively. Adding the respective volumes of water indicates the total volumes of TCE and water in CBV-300, CBV-720, and CBV-780 are 0.41, 0.36, and 0.30

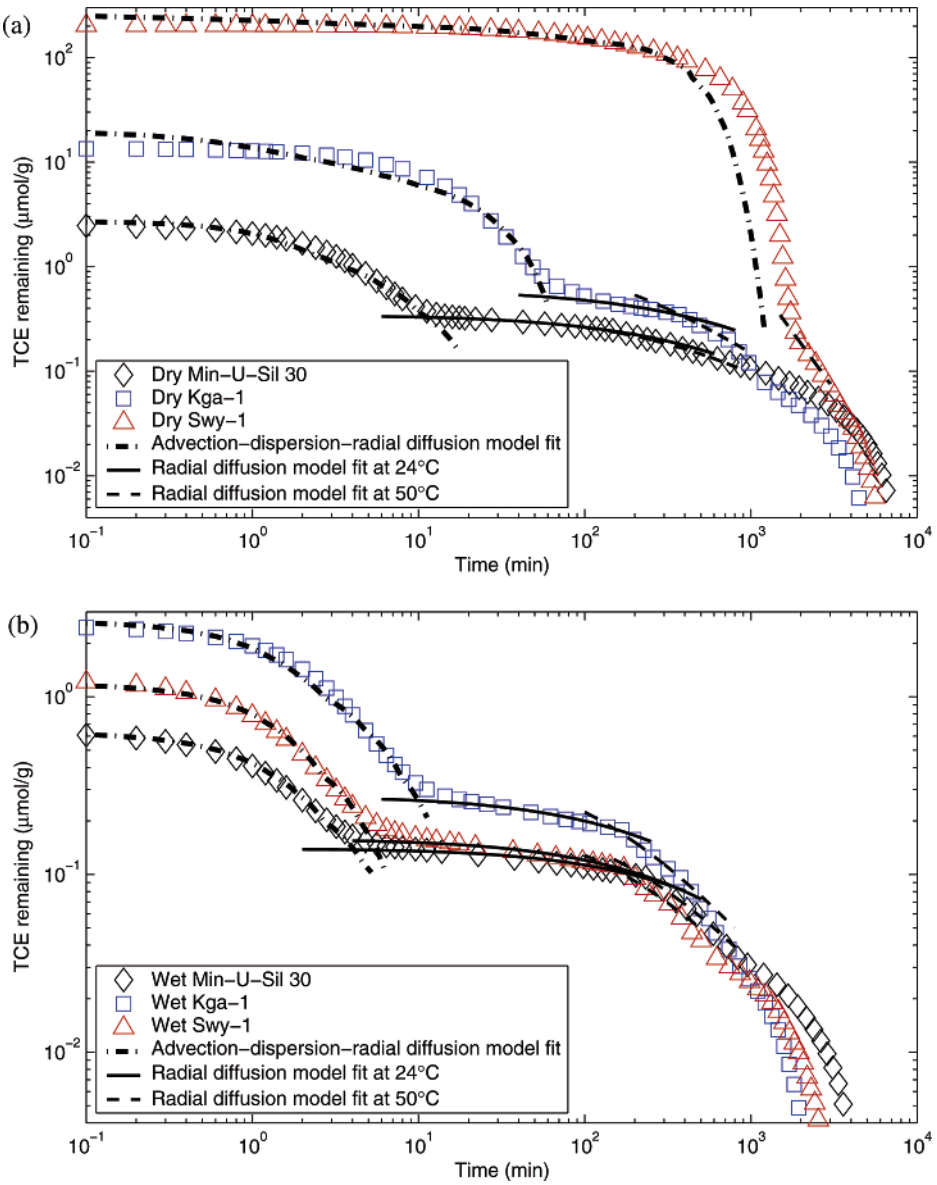


**FIGURE 4. Desorption of TCE from three natural minerals under (a) dry and (b) wet conditions, along with the model-fitted desorption profiles. Stepwise increases in desorption temperature were made to accelerate the desorption rate, with the model-fitted desorption profiles at 50 °C also shown.**

mL/g, respectively, corresponding to 91.3%, 81.1%, and 68.0% pore filling. In calculating the total filled pore volumes, it was assumed that TCE (and helium) did not displace coordinated water. In partially dehydrated zeolites, TCE presumably interacts mainly through dispersion interactions with pore wall surfaces and dipole interactions with surface cations that were not fully hydrated. CBV-720 (3.71 mmol/g) sorbed a larger amount of TCE than CBV-780 (3.13 mmol/g), possibly because cations with unfilled coordination shells attracted additional TCE molecules.

For wet CBV-300, the amount of TCE that resided in the interparticulate void spaces, sorbed on external surfaces, and partitioned in the water film was no longer negligible compared to that sorbed in the micropores. Consequently, TCE sorbed in micropores of wet CBV-300 was quantified from the slow-desorbing fraction (data not shown). TCE sorption increased with decreasing surface cation density from $1.72 \times 10^{-3}$ to 0.85 and 0.93 mmol/g for CBV-300, CBV-720, and CBV-780, respectively. Compared to partially dehydrated conditions, TCE sorption was much smaller in all cases, which was apparently caused by the strong competition from water for sorption space. On CBV-720 and CBV-780, the sums of the volumes of TCE after TCE sorption and the volumes of water before TCE sorption exceeded the total micropore volumes. The fact that TCE is taken up by water-filled micropores can only be explained by TCE displacing water. Alternative explanations include expansion of the crystalline framework of zeolites and compression of TCE and water, which appear unlikely. At 24 °C and a relative pressure of 0.136 ($5.05 \times 10^{-1}$ mmol/L), TCE occupied only 0.034% of the total micropore volume in wet CBV-300, but 16.9% and 18.6% in wet CBV-720 and CBV-780, respectively.

Taken together, these results indicate that the absence of hydrophilic sites, i.e., the hydrophobicity of the micropores, is a controlling factor in the uptake of organic compounds. CBV-720 and CBV-780 have relatively low densities of hydrophilic centers (cation density 0.42 and 0.16 site/nm$^2$) and the pore water is largely loosely bound, allowing significant TCE adsorption. In contrast, very little water was loosely bound in the micropores of wet CBV-300 (cation density 2.07 sites/nm$^2$), and the amount of TCE adsorbed was much smaller. These findings agree with the molecular simulation results of carbon micropores, which show that sorption of methane increases while that of water

decreases with increasing density of hydrogen-bonding sites (*17*, *20*).

**TCE Desorption from Silica Sand, Kaolinite, and Smectite.** Figure 4 shows TCE mass remaining profiles from dry and wet Min-U-Sil 30, KGa-1, and SWy-1, along with the model fits for differentiation of the fast- and slow-desorbing fractions. TCE was sorbed on the external surfaces and to a smaller extent in the micropores on the dry solids. Inflection points were noted on the mass remaining profiles of dry Min-U-Sil 30 and KGa-1 (Figure 4a), suggesting the onset of slow desorption from micropores. In contrast, no clear transition from fast to slow desorption was observed on dry SWy-1. It is possible that TCE adsorbed on the external surfaces also contributed significantly to slow desorption (*5*), making quantification of the flux desorbed from micropores difficult on dry SWy-1. Nonetheless, it is reasonable to assume that most of the TCE desorbed after 100−1000 min originated from the micropores. From the approximate transition points, the amounts of TCE sorbed in the micropores of dry Min-U-Sil 30, KGa-1, and SWy-1 were estimated to be 0.34 (at 15 min), $6.1 \times 10^{-4}$ (at 75 min), and $2.67 \times 10^{-2}$ (at 1000 min) to $1.54 \times 10^{-1}$ (at 100 min) mmol/g, corresponding to (total) micropore volumes of $3.0 \times 10^{-2}$, $5.5 \times 10^{-2}$, and 2.4−13.9 $\mu$L/g, respectively.

Under wet conditions, the fast to slow desorption transition was distinct in all cases (Figure 4b), and the desorption data were evaluated similarly. Removal of the fast-desorbing TCE occurred in less than 10 min, and the contribution from micropore desorption was negligible. The slow-desorbing TCE masses were $1.5 \times 10^{-4}$, $3.0 \times 10^{-4}$, and $1.8 \times 10^{-4}$ mmol/g, corresponding to hydrophobic micropore volumes of 1.4 $\times 10^{-2}$, 2.7 $\times 10^{-2}$, and 1.7 $\times 10^{-2}$ $\mu$L/g in Min-U-Sil 30, KGa-1, and SWy-1, respectively. The hydrophobic micropores are believed to exist in the micropore spaces surrounded by uncharged siloxane surfaces (*5*, *26*). Such hydrophobic micropores may play an important role in hydrophobic contaminant sorption. For example, for low organic carbon (<0.1%) aquifer materials from the Borden site, important fractions of their sorption capacities and the slow sorption kinetics have been attributed to micropores (*30*). Strong uptake of phenanthrene from water by smectites has also been attributed to capillary condensation into the network of micropores created by the quasicrystals or tactoids of clay (*31*).

The above results indicate that the organic sorption capacity of microporous sorbents is determined by both the total volume and hydrophobicity of the micropores, consistent with the observations made on zeolites. Min-U-Sil 30 exhibited the lowest micropore sorption capacities for TCE sorption under dry ($3.4 \times 10^{-4}$ mmol/g) and wet ($1.5 \times 10^{-4}$ mmol/g) conditions, as expected on the basis of its low microporosity and mostly uncharged surfaces. KGa-1 sorbed a relatively small amount of TCE ($6.1 \times 10^{-4}$ mmol/g) under dry conditions because kaolinites have relatively low total microporosity (*23*, *24*); the relatively large amount of TCE ($3.0 \times 10^{-4}$ mmol/g) sorbed under wet conditions is explained by uncharged siloxane surfaces creating hydrophobic micropore spaces. Under dry conditions, micropores of SWy-1 sorbed the highest amount of TCE ($2.68 \times 10^{-2}$ to $1.54 \times 10^{-1}$ mmol/g), but only a relatively small amount ($1.8 \times 10^{-4}$ mmol/g) under wet conditions. This can be explained by its predominantly hydrophilic micropores caused by the high layer charge (−0.68 per unit cell) (*32*). Taken together, these results suggest that minerals can contribute substantially to the microporosity of geosorbents. For a low organic carbon (0.11%) sediment composed of quartz, albite, smectite, and kaolinite, we previously determined that $5.17 \times 10^{-2}$ and $3.0 \times 10^{-4}$ mmol/g TCE sorbed in its micropores under dry and wet conditions, corresponding to total and hydrophobic micropore volumes of 4.65 and $2.7 \times 10^{-2}$ $\mu$L/g, respectively (*5*). These values are consistent with microporosity contributed mostly from geosorbent minerals.

**Implications on VOC Sorption in Geosorbents.** Results of this study suggest that TCE adsorbs in hydrophobic mineral micropores through displacing loosely bound water and that the total uptake is controlled by the volume and hydrophobicity of micropores. These conclusions are consistent with and support experimental, thermodynamic, and modeling results presented by others (*3*, *17*, *20*, *21*, *26*). Further corroboration of the displacement mechanism requires a mass balance for water, which was outside the scope of this study. Results also indicate that hydrophobic micropores in silicate minerals of geosorbents alone can cause substantial sorption of VOCs. The estimated apparent partitioning coefficients of TCE in the micropores of Min-U-Sil 30, KGa-1, and SWy-1 are 0.13, 0.27, and 0.16 L/kg (Supporting Information), which are equivalent to organic carbon contents of 0.10%, 0.20%, and 0.12%, respectively. These results support the conclusion from previous studies that the mineral matrix can play an important role in VOC sorption on geosorbents with low (<0.1%) organic carbon contents (*33*−*35*). Therefore, characterization of the geosorbent mineral matrix is necessary for understanding organic contaminants transport in subsurface soils and groundwater aquifers having geosorbents with low organic carbon contents.

## Acknowledgments

This study was funded by the U.S. EPA under Project R828772-01 through the Western Region Hazardous Substance Research Center. We thank Dr. Istvan Halasz at PQ Corp. for discussions on the structure of dealuminated Y zeolites and anonymous reviewers for helpful comments.

## Supporting Information Available

Additional information on zeolite dealumination and crystallinity of the dealuminated Y zeolites, FAU structure, displacement of loosely bound water by TCE in a hydrophobic micropore, zeolite dehydration, effect of sample preparation on structures and surface properties of the zeolites and natural minerals, micropore formation in the natural minerals, micropore desorption rate constants, and estimation for the apparent partitioning coefficients of TCE. This material is available free of charge via the Internet at http://pubs.acs.org.

## Literature Cited

(1) Farrell, J.; Reinhard, M. Desorption of halogenated organics from model solids, sediments, and soil under unsaturated conditions. 2. Kinetics. *Environ. Sci. Technol.* **1994**, *28* (1), 63−72.
(2) Werth, C. J.; Reinhard, M. Effects of temperature on trichloroethylene desorption from silica gel and natural sediments. 2. Kinetics. *Environ. Sci. Technol.* **1997**, *31* (3), 697−703.
(3) Farrell, J.; Manspeaker, C.; Luo, J. Understanding competitive adsorption of water and trichloroethylene in a high-silica Y zeolite. *Microporous Mesoporous Mater.* **2003**, *59* (2−3), 205−214.
(4) Li, J.; Werth, C. J. Slow desorption mechanisms of volatile organic chemical mixtures in soil and sediment micropores. *Environ. Sci. Technol.* **2004**, *38* (2), 440−448.
(5) Cheng, H.; Reinhard, M. Measuring hydrophobic micropore volumes in geosorbents from trichloroethylene desorption data. *Environ. Sci. Technol.* **2006**, *40* (11), 3595−3602.
(6) Aringhieri, R. Nanoporosity characteristics of some natural clay minerals and soils. *Clays Clay Miner.* **2004**, *52* (6), 700−704.
(7) Breck, D. W. *Zeolite Molecular Sieves, Structure, Chemistry and Use*; John Wiley: New York, 1974.
(8) Chen, N. Y. Hydrophobic properties of zeolites. *J. Phys. Chem.* **1976**, *80* (1), 60−64.
(9) Kerr, G. T. Intracrystalline rearrangement of constitutive water in hydrogen zeolite Y. *J. Phys. Chem.* **1967**, *71* (12), 4155−4156.
(10) Ruthven, D. M. *Principles of Adsorption and Adsorption Processes*; John Wiley: New York, 1984.

(11) Leherte, L.; Andre, J. M.; Derouane, E. G.; Vercauteren, D. P. Self-diffusion of water into a ferrierite-type zeolite by molecular dynamics simulations. *J. Chem. Soc., Faraday Trans.* **1991**, *87* (13), 1959−1970.
(12) Brauner, K.; Preisinger, A. Struktur und Entstehung des Sepioliths. *Tschermaks Mineral. Petrogr. Mitt.* **1956**, *6*, 120−140.
(13) Gregg, S. J.; Sing, K. S. W. *Adsorption, Surface Area and Porosity*; Academic Press: London, 1982.
(14) van Reeuwijk, L. P. *The thermal dehydration of natural zeolites*; H. Veenmanand Zonen B.V.: Wageningen, The Netherlands, 1974.
(15) Majzlan, J.; Lang, B. E.; Stevens, R.; Navrotsky, A.; Woodfield, B. F.; Boerio-Goates, J. Thermodynamics of Fe oxides: Part I. Entropy at standard temperature and pressure and heat capacity of goethite (alpha-FeOOH), lepidocrocite (gamma-FeOOH), and maghemite (gamma-$Fe_2O_3$). *Am. Mineral.* **2003**, *88* (5−6), 846−854.
(16) Ruiz-Hitzky, E. Molecular access to intracrystalline tunnels of sepiolite. *J. Mater. Chem.* **2001**, *11* (1), 86−91.
(17) Muller, E. A.; Gubbins, K. E. Molecular simulations study of hydrophilic and hydrophobic behavior of activated carbon surfaces. *Carbon* **1998**, *36* (10), 1433−1438.
(18) Shevade, A. V.; Jiang, S.; Gubbins, K. E. Adsorption of water-methanol mixtures in carbon and alumino-silicate pores: a molecular simulation study. *Mol. Phys.* **1999**, *97* (10), 1139−1148.
(19) Muller, E. A.; Rull, L. F.; Vega, L. F.; Gubbins, K. E. Adsorption of water on activated carbons: A molecular simulation. study. *J. Phys. Chem.* **1996**, *100* (4), 1189−1196.
(20) Muller, E. A.; Hung, F. R.; Gubbins, K. E. Adsorption of water vapor-methane mixtures on activated carbons. *Langmuir* **2000**, *16* (12), 5418−5424.
(21) Luo, J.; Farrell, J. Examination of hydrophobic contaminant adsorption in mineral micropores with grand canonical Monte Carlo simulations. *Environ. Sci. Technol.* **2003**, *37* (9), 1775−1782.
(22) Aylmore, L. A. G.; Quirk, J. P. Domain of turbostratic structure of clays. *Nature* **1960**, *187* (4742), 1046−1048.
(23) Quirk, J. P.; Aylmore, L. A. G. Domains and quasi-crystalline regions in clay systems. *Soil Sci. Soc. Am. Proc.* **1971**, *35* (4), 652−654.
(24) Murray, R. S.; Quirk, J. P. Surface area of clays. *Langmuir* **1990**, *6* (1), 122−124.
(25) Neaman, A.; Pelletier, M.; Villieras, F. The effects of exchanged cation, compression, heating and hydration on textural properties of bulk bentonite and its corresponding purified montmorillonite. *Appl. Clay Sci.* **2003**, *22* (4), 153−168.
(26) Farrell, J.; Hauck, B.; Jones, M. Thermodynamic investigation of trichloroethylene adsorption in water-saturated microporous adsorbents. *Environ. Toxicol. Chem.* **1999**, *18* (8), 1637−1642.
(27) Schwarzenbach, R. P.; Gschwend, P. M.; Imboden, D. M. *Environmental Organic Chemistry*; John Wiley & Sons: New York, 2002.
(28) Halasz, I.; Kim, S.; Marcus, B. Hydrophilic and hydrophobic adsorption on Y zeolites. *Mol. Phys.* **2002**, *100* (19), 3123−3132.
(29) Dhingra, O. D.; Sinclair, J. B. *Basic Plant Pathology Methods*, 2nd ed.; CRC Press: Boca Raton, FL, 1995.
(30) Ball, W. P.; Roberts, P. V. Long-term sorption of halogenated organic chemicals by aquifer material. 2. Intraparticle diffusion. *Environ. Sci. Technol.* **1991**, *25* (7), 1237−1249.
(31) Hundal, L. S.; Thompson, M. L.; Laird, D. A.; Carmo, A. M. Sorption of phenanthrene by reference smectites. *Environ. Sci. Technol.* **2001**, *35* (17), 3456−3461.
(32) Jaynes, W. F.; Bigham, J. M. Charge reduction, octahedral charge, and lithium retention in heated, Li-saturated smectites. *Clays Clay Miner.* **1987**, *35* (6), 440−448.
(33) McCarty, P. L.; Reinhard, M.; Rittmann, B. E. Trace organics in groundwater. *Environ. Sci. Technol.* **1981**, *15* (1), 40−51.
(34) Schwarzenbach, R. P.; Westall, J. C. Transport of nonpolar organic compounds from surface water to groundwater. Laboratory sorption studies. *Environ. Sci. Technol.* **1981**, *15* (11), 1360−1367.
(35) Curtis, G. P.; Roberts, P. V.; Reinhard, M. A natural gradient experiment on solute transport in a sand aquifer. 4. Sorption of organic solutes and its influence on mobility. *Water Resour. Res.* **1986**, *22* (13), 2059−2067.
(36) van Olphen, H.; Fripiat, J. J. *Data Handbook of Clay Materials and Other Non-Metallic Minerals*; Pergamon Press: New York, 1979.
(37) Chipera, S. J.; Bish, D. L. Baseline studies of the Clay Minerals Society source clays: powder X-ray diffraction analyses. *Clays Clay Miner.* **2001**, *49* (5), 398−409.
(38) Breiner, J. M.; Anderson, M. A.; Tom, H. W. K.; Graham, R. C. Properties of surface-modified colloidal particles. *Clays Clay Miner.* **2006**, *54* (1), 12−24.

*Received for review April 12, 2006. Revised manuscript received September 19, 2006. Accepted September 20, 2006.*

ES060886S